Journal of Hazardous Materials 161 (2009) 1140–1149

Contents lists available at ScienceDirect

Journal of Hazardous Materials

journal homepage: www.elsevier.com/locate/jhazmat

Biodegradation of 2,4,6-trichlorophenol in a packed-bed biofilm reactor equipped with an internal net draft tube riser for aeration and liquid circulation

A. Gómez-De Jesús, F.J. Romano-Baez, L. Leyva-Amezcua, C. Juárez-Ramírez, N. Ruiz-Ordaz, J. Galíndez-Mayer*

Departamento de Ingeniería Bioquímica, Escuela Nacional de Ciencias Biológicas, IPN. Prol. Carpio y Plan de Ayala, Colonia Santo Tomás, s/n. CP 11340, México, D.F., Mexico

ARTICLE INFO

Article history:
Received 3 August 2007
Received in revised form 7 April 2008
Accepted 21 April 2008
Available online 26 April 2008

Keywords:
Airlift reactor
Cometabolism
Packed-bed reactor
Stenotrophomonas
Trichlorophenol

ABSTRACT

For the aerobic biodegradation of the fungicide and defoliant 2,4,6-trichlorophenol (2,4,6-TCP), a bench-scale packed-bed bioreactor equipped with a net draft tube riser for liquid circulation and oxygenation (PB-ALR) was constructed. To obtain a high packed-bed volume relative to the whole bioreactor volume, a high A_D/A_R ratio was used. Reactor's downcomer was packed with a porous support of volcanic stone fragments. PB-ALR hydrodynamics and oxygen mass transfer behavior was evaluated and compared to the observed behavior of the unpacked reactor operating as an internal airlift reactor (ALR). Overall gas holdup values ε_G, and zonal oxygen mass transfer coefficients determined at various airflow rates in the PB-ALR, were higher than those obtained with the ALR. When comparing mixing time values obtained in both cases, a slight increment in mixing time was observed when reactor was operated as a PB-ALR.

By using a mixed microbial community, the biofilm reactor was used to evaluate the aerobic biodegradation of 2,4,6-TCP. Three bacterial strains identified as *Burkholderia* sp., *Burkholderia kururiensis* and *Stenotrophomonas* sp. constituted the microbial consortium able to cometabolically degrade the 2,4,6-TCP, using phenol as primary substrate. This consortium removed 100% of phenol and near 99% of 2,4,6-TCP. Mineralization and dehalogenation of 2,4,6-TCP was evidenced by high COD removal efficiencies (≈95%), and by the stoichiometric release of chloride ions from the halogenated compound (≈80%). Finally, it was observed that the microbial consortium was also capable to metabolize 2,4,6-TCP without phenol as primary substrate, with high removal efficiencies (near 100% for 2,4,6-TCP, 92% for COD and 88% for chloride ions).

1. Introduction

Biofilm reactors are increasingly used in place of suspended growth bioreactors because of their resistance to short-term toxic loads, the ability of the attached biomass to survive at low influent substrate concentrations (oligotrophic conditions), and their high volumetric biomass concentrations, which allow small reactor volumes [1]. However, in aerobic packed-bed bioreactors the low solubility of oxygen in water, joined to their uninterrupted microbial consumption, turns the oxygen transfer rate in a design key factor in aerobic packed-bed reactors (PBRs). To sustain active immobilized biomass uniformly distributed within the PBR, a continuous and homogeneous supply of oxygen and substrates must be ensured via high liquid circulation and oxygen transfer rates. Devices such as airlift pumps, consuming small amounts of energy for liquid oxygenation and distribution through the packed bed, could improve the process economy.

In this work, a packed-bed bioreactor with a net draft tube for liquid aeration and mixing was constructed, evaluating its hydrodynamics and mass transfer performance; as well as its performance as an attached biofilm reactor for 2,4,6-trichlorophenol degradation.

1.1. Packed-bed reactors

Packed-bed aerobic reactors are widely used for wastewater treatment. It has been demonstrated that PBRs could resist higher concentrations of toxic compounds, leading to superior removal rates than suspended growth reactors [2]. PBRs' usual flow possibilities are up-flow or down-flow in single or multiple pass (recycling), with the fluids moving axially to the bed height in concurrent or

* Corresponding author. Tel.: +52 5729 6000x62352; fax: +52 5396 3503.
E-mail addresses: cmayer@encb.ipn.mx, juvenciogm@yahoo.com (J. Galíndez-Mayer).

0304-3894/$ – see front matter © 2008 Elsevier B.V. All rights reserved.
doi:10.1016/j.jhazmat.2008.04.077

Nomenclature

A_D downcomer sectional area (cm^2)
A_R riser sectional area (cm^2)
$B_{V,COD} = (F_L C_{COD})/V_L$ volumetric loading rate of COD ($mg\,L^{-1}\,h^{-1}$)
$B_{V,Phe} = (F_L C_{Phe})/V_L$ volumetric loading rate of phenol ($mg\,L^{-1}\,h^{-1}$)
$B_{V,TCP} = (F_L C_{TCP})/V_L$ volumetric loading rate of 2,4,6-TCP ($mg\,L^{-1}\,h^{-1}$)
$\tilde{c}_{Cl}$ chloride concentration in the outgoing medium ($mg\,L^{-1}$)
$\tilde{c}_{COD}$ COD concentration in the outgoing medium ($mg\,L^{-1}$)
C_{COD} COD concentration in the inflowing medium ($mg\,L^{-1}$)
$\tilde{c}_{Phe}$ phenol concentration in the outgoing medium ($mg\,L^{-1}$)
$\tilde{c}_{TCP}$ TCP concentration in the outgoing medium ($mg\,L^{-1}$)
CFU colony forming unit
Cl_{in} chloride concentration in the inflowing medium ($mg\,L^{-1}$)
C_L DO concentration in liquid phase ($mg\,L^{-1}$)
C_{Phe} phenol concentration in the inflowing medium ($mg\,L^{-1}$)
C_S dissolved oxygen concentration at equilibrium ($mg\,L^{-1}$)
C_{TCP} TCP concentration in the inflowing medium ($mg\,L^{-1}$)
d_P particle diameter (cm)
$D = F_L/V_L$ reactor's dilution rate (d^{-1})
d_{BSM} Sauter mean diameter (cm)
D_C column diameter (cm)
D_R riser diameter (cm)
F_L liquid flow rate ($L\,d^{-1}$)
H_{PB} height of the packed bed (cm)
$k_L a_D$ mass transfer coefficient in downcomer (h^{-1})
$k_L a_R$ mass transfer coefficient in riser (h^{-1})
M_{PB} Mass of support material in packed bed (g)
Q_{AIR} gas flow rate ($L\,min^{-1}$)
$R_{V,COD} = F_L(C_{COD} - \tilde{c}_{COD})/V_L$ volumetric degradation rate of COD ($mg\,L^{-1}\,d^{-1}$)
$R_{V,Phe} = F_L(C_{Phe} - \tilde{c}_{Phe})/V_L$ volumetric degradation rate of phenol ($mg\,L^{-1}\,d^{-1}$)
$R_{V,TCP} = F_L(C_{TCP} - \tilde{c}_{TCP})/V_L$ volumetric degradation rate of 2,4,6-TCP ($mg\,L^{-1}\,d^{-1}$)
$R_{X,TCP} = F_L(C_{TCP} - \tilde{c}_{TCP})/(V_{void}\rho_{TZ}X_{PB})$ specific degradation rate of 2,4,6-TCP ($mg\,(10^9\ CFU)^{-1}\,d^{-1}$)
t_{m95} time to reach 95% homogeneity after a tracer input (s)
U_{GR} superficial air velocity in riser ($cm\,s^{-1}$)
$V_C = V_D + V_R$ column volume (L)
V_D downcomer volume (L)
$V_L = V_{void} + V_R$ reactor's liquid volume (L)
V_{LS} reactor operational volume (L)
V_P particle volume (cm^3)
$V_{PB} = V_D$ packed-bed volume (L)
V_R riser volume (L)
$V_{void} = V_{PB}(\varepsilon_e + \varepsilon_p)$ void volume of packed-bed (L)
X_{PB} attached cells concentration ($CFU\,(g\ dry\ support)^{-1}$)

Greek letters
$\Delta pH[t] = (pH_0 - pH[t])/(pH_0 - pH_\infty)$ relative pH change
ε_e inter particle porosity
ε_p intra particle porosity
$\varepsilon_{tot} = \varepsilon_e + \varepsilon_p$ total bed porosity
ε_L liquid hold-up (%)
ε_G gas hold-up (%)
$\eta_{Cl} = (Cl_{in} - \tilde{c}_{Cl})/Cl_{in}$ dechlorination efficiency (%)
$\eta_{COD} = (C_{COD} - \tilde{c}_{COD})/C_{COPD}$ COD removal efficiency (%)
$\eta_{Phe} = (C_{Phe} - \tilde{c}_{Phe})/C_{Phe}$ phenol removal efficiency (%)
$\eta_{TCP} = (C_{TCP} - \tilde{c}_{TCP})/C_{TCP}$ TCP removal efficiency (%)
$\theta_R = 1/D$ hydraulic retention time (d)
ρ_{TZ} dry support material density ($g\,cm^{-3}$)

Subscripts
B bottom
C column
D downcomer
G gas
L liquid
PB packed-bed
R riser
S solid
T top
V volumetric

countercurrent flow. When operated as downward gas–liquid flow packed beds, the liquid flow is laminar. When PBRs are up-flow-concurrently operated, bubbly flow occurs at low gas-flow rates and poor oxygen transfer coefficients are obtained. If the gas flow is increased further, slug flow occurs and gas channeling leads to the development of liquid-rich and gas-rich regions [3]. In both operation modes, countercurrent or concurrent downward trickle-flow regime, packed-bed reactors present low liquid holdup. In countercurrent mode, gas/liquid flow-rate ratio is restricted by the flooding limit. Heterogeneity could be an important disadvantage, i.e. concentration and cell gradients over the fixed bed height and within the biofilm attached to support, or the strongly heterogeneous $k_L a$ coefficients observed along PBR vertical axis [4]. Another disadvantage of PBRs is the pressure drop which is influenced by variables such as: bed height, support porosity, particle diameter and superficial fluid velocity [5,6]. To reduce heterogeneity and pressure drop, favoring oxygen mass transfer and liquid mixing through the porous support, the aforementioned variables were considered to construct a bench-scale recycling packed-bed bioreactor for the aerobic degradation of recalcitrant water pollutants.

For the successful application of any material as support in fixed film stationary bed reactors, Jördening and Buchholz [7], recommend that the following general requirements should be fulfilled: availability of the material in big quantities, low cost, inert behavior (mechanically and microbiologically stable), and showing low pressure drop. Thus, a kind of vesicular volcanic-scoria broadly distributed in central México (tezontle) satisfying the aforementioned requirements, was used as packed-bed biofilm support.

The liquid recycling is advantageous for biodegradation of recalcitrant soluble substrates, because linear velocity of substrate solution and packed-bed height affect the hydraulic retention time and thus the biodegradation efficiency. Liquid recycling allows the substrate solution to be passed through the column at a desired velocity. Unless high recycling rates are used, concentration gradients will be formed in packed-bed biofilm reactors, affecting the global biodegradation rate. However, fluid recycling augments pressure drop across the packed bed or column, increasing the operational costs of the degradation bioprocess. Since cross flow design in packed beds reduces pressure drop enabling the use of

practical flow rates and even flow distribution across wide packed bed [8], the PB-ALR prototype was constructed to operate with axial and radial flow. In this bioreactor, oxygen mass transfer limitations were attenuated by oxygenating the liquid in a wire-mesh draft tube located in the center of the packed bed. The net draft tube operated as an airlift pump, delivering the oxygenated liquid through the packed bed and circulating it radially to the riser [9].

1.2. Biodegradation of 2,4,6-trichlorophenol

Chlorophenolic compounds are toxic pollutants widely distributed in aquatic environments [10]. Polychlorinated phenols such as 2,4,6-trichlorophenol are recalcitrant compounds that present toxic effects on aquatic biota [11], and whose extended use in agriculture and industry has resulted in severe environmental contamination [12]. Among the six trichlorophenol isomers, the 2,4,5- and 2,4,6-ones have been placed on the US Environmental Protection Agency's priority pollutants list [13]. In the European Community, 2,4,6-TCP has been included in directive 76/464/EEC as a dangerous substance discharged into the aquatic environment [14]. 2,4,6-TCP (CAS#88062) is a breakdown product of pesticides such as: pentachlorophenol, lindane and hexacholorobenzene, and it is one of the main components of the bleached Kraft pulp mill effluents. It is widely used as a fungicide, defoliant agent, disinfectant and preservative [15,16].

Removal and detoxification of chlorophenols to improve the quality of water can be achieved by chemical or physical methods [17–19]. However, microbial biodegradation could provide a cost-effective and environmentally safe way to remove them from contaminated environments. Attention has been devoted to the use of anaerobic treatment systems for biodegradation of highly chlorinated phenols [20]. Although bacterial species able to anaerobically degrade 2,4,6-TCP as the only carbon and energy sources can be attained [12], their cometabolic biodegradation in aerobic conditions can also be achieved [21,22]. Furthermore, aerobic bacterial strains have been reported to degrade this pollutant using it as the sole carbon and energy source [23–26]. Aerobic biodegradation of 2,4,6-TCP by suspended microbial communities has been informed [27]. However, it has been reported that a defined mixed community able to degrade 2,4,6-TCP in suspended cell culture, shows inability to effectively degrade it when growing in a conventional packed-bed biofilm reactor [28]. In this case, authors concluded that their PBR resulted unsuitable for oxygen-sensitive bacteria, suggesting the use of another reactor system supplying sufficient oxygen to treat 2,4,6-TCP.

2. Experimental

2.1. Chemicals

All components used in culture media were obtained from Merck (Darmstadt, Germany). Phenol (Phe) and 2,4,6-trichlorophenol (2,4,6-TCP), were acquired from Sigma–Aldrich (USA). The solvents used for HPLC were purchased from J.T. Baker (USA).

2.2. Microorganisms

By using a chemostat fed with phenol plus 2,4,6-TCP, a mixed microbial culture able to cometabolically degrade 2,4,6-TCP was selected from microbial communities isolated in several contaminated sites of Central México [29]. The mixed microbial culture was composed by three bacterial species. By PCR amplification, sequencing of bacterial 16S rDNA amplicons, and comparison with known sequences of 16S rDNA from the NCBI GenBank, the bacterial strains were identified as: *Stenotrophomonas* sp. with accession number: AY563052 [97% similarity], *Burkholderia kururiensis* with accession number: EF178438 [96% similarity], and *Burkholderia tropica* with accession number: EF139183 [91% similarity]. Reported species with the best similarity matches were regarded as the isolated species. Because of the low similarity of the second *Burkholderia* strain, compared to the *Burkholderia tropica* strain reported in the GenBank database, it was denominated as *Burkholderia* sp. When individual bacterial strains were inoculated in mineral salt medium with 2,4,6-TCP as the sole carbon and energy source, no growth was appreciated. Scarce growth was observed when individual bacterial strains were cultivated on 2,4,6-TCP plus phenol. However, when the mixed bacterial culture was grown on mixed substrates, a noteworthy increase in growth rate was observed, thus, the biological test of the PBR-AL was made using these last conditions.

2.3. Mineral salts (MS) medium

The media composition (in $g\,L^{-1}$) was: KNO_3, 0.35; $(NH_4)_2SO_4$, 0.25; KH_2PO_4, 0.20; $MgSO_4$, 0.10; $Ca(NO_3)_2.4H_2O$, 0.04; $MnSO_4$, 1.6 $mg\,L^{-1}$; Na_2MoO_4, 0.8 $mg\,L^{-1}$. As carbon and energy sources, 2,4,6-TCP or 2,4,6-TCP plus phenol were added in different concentrations. Microorganisms were maintained in agar slants with MS medium supplemented with phenol (100 $mg\,L^{-1}$) plus 2,4,6-TCP (50 $mg\,L^{-1}$).

2.4. Packed-bed biofilm support

Tezontle is a vesicular basaltic-andesitic-scoria accumulated in the Trans-Mexican Volcanic Belt by Strombolian volcanic eruptions. This material is broadly distributed in central México and is widely used in construction industry. His name proceeds from the nahuatl word *tetzontli* (from *tetl*, stone, and *tzontli*, hair). This volcanic stone was used as packed-bed biofilm support. The non-uniform rough particles of tezontle has a porous microstructure; consequently, the fluid in their interior is considered stagnant and intra-particular mass transfer occurs by diffusion. Because packings of less than 3 mm diameter can lead to excessive pressure drop [2], irregular volcanic stone fragments exceeding this value were used as packing in the PB-ALR. Porous fragments were considered as ellipsoid bodies with three characteristic radii: *a*, *b* and *c*. Using the equation

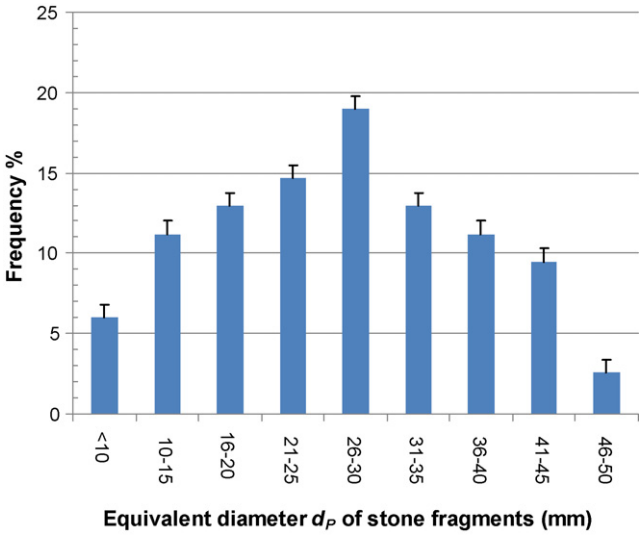

Fig. 1. Size distribution of the porous stone fragments.

Table 1
Characteristics of the packed-bed support constituted by porous volcanic stone

Intra-particle porosity of volcanic stone, ε_p	0.273
Inter-particle porosity of volcanic stone, ε_e	0.455
Total bed porosity, $\varepsilon_{tot} = \varepsilon_e + \varepsilon_p$	0.728
Dry material bulk density, ρ_{TZ} (g cm^{-3})	2.385
Packed-bed volume, V_{PB} (cm^3)	4628
Packed-bed void volume, $V_{void} = V_{PB}(\varepsilon_e + \varepsilon_p)$ (cm^3)	3369
Packed-bed circulating liquid volume, $V_{PB}(\varepsilon_e)$ (cm^3)	2106
Packed-bed stagnant liquid volume, $V_{PB}(\varepsilon_p)$ (cm^3)	1263

$$V_P = \frac{4\pi}{3}abc,$$

the particle volume V_P was calculated and used to obtain the equivalent diameter d_P of spherical particles from the equation

$$d_P = \left[\frac{6V_P}{\pi}\right]^{1/3}$$

Size distribution of the porous volcanic stone and packed-bed characteristics are shown in Fig. 1 and Table 1, respectively. Porosity of volcanic stone was determined according to the method described by Hodge and Devinny [30].

2.5. Bioreactor

The lab-scale fixed-bed reactor (Fig. 2) used in this study was composed by three flanged glass modules joined with metallic clamps and sealed with neoprene gaskets. The lower module holds a porous glass diffuser located at the center of a stainless steel wire-mesh draft tube supported by an external rigid PVC framework allowing the free liquid flow between downcomer and riser. The central module is the reactor's body that contains the porous packed bed. The third module is reactor's cover which has entries for acid or alkali addition, for pH and DO electrodes, for liquid medium input, and for air venting.

Although in conventional airlift reactors (ALR) the value of the volumetric mass transfer coefficient k_La decreases when the A_D/A_R ratio is increased [31], in order to reduce pressure drop, and to have a high packed-bed volume in the downcomer relative to the volume of the whole bioreactor, and consequently higher amounts of reactive biomass, a low H_{PB}/D_C (1.22) and a high A_D/A_R (10.7) ratios were used for the PB-ALR.

The prototype operated as a recirculating packed-bed reactor with two delimited zones. In the first one (wire-mesh tube riser), liquid is oxygenated and flows upward to the second zone where it is distributed through the packed bed, delivering the absorbed O_2 to the microbial biofilm attached to the material support. Finally, the exhausted liquid radially returns to the net draft tube riser.

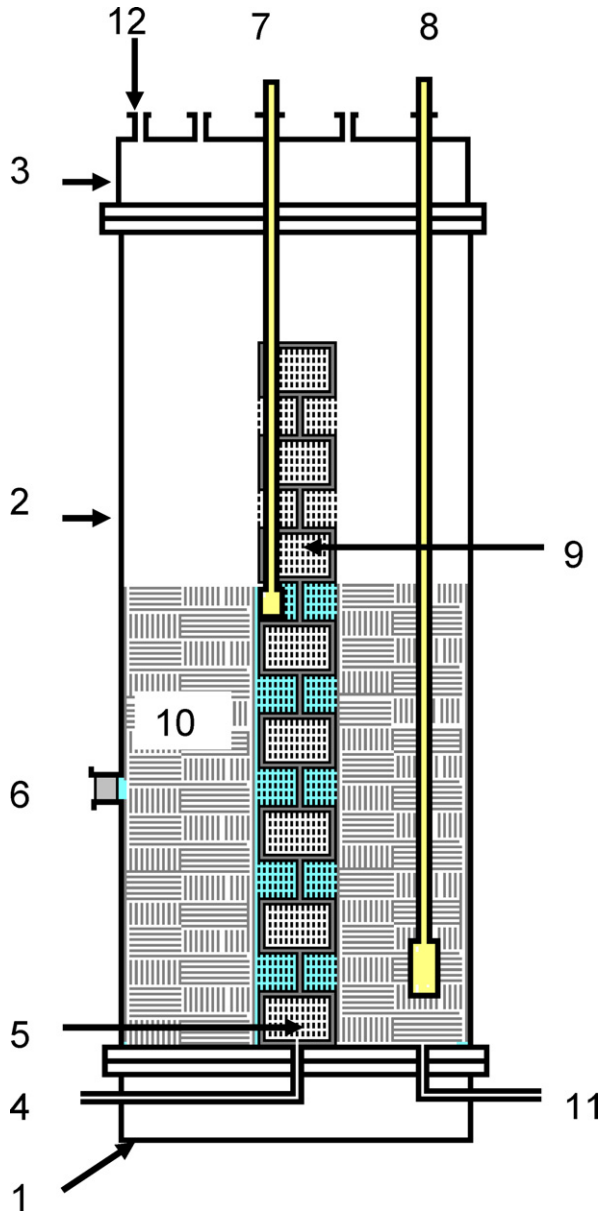

Fig. 2. PB-ALR configuration. Lower (1), central (2) and top (3) reactor's modules; air input (4); porous glass diffuser (5); port for tracer injection (6); pH or DO electrode at riser (7); pH or DO electrode at downcomer (8); stainless-steel wire-mesh draft tube supported by an external rigid-PVC framework (9); porous packed bed (10); reactor's drain (11); liquid medium input (12).

2.6. Bioreactor hydrodynamics

2.6.1. Mixing time (t_{m95}) in packed or unpacked bioreactor

Mixing time was determined using a tracer technique that measures pH change in a prehomogenized solution after an acid pulse. Two pH electrodes were used, one of them was located in the middle of the riser, and the other in the lower part of the downcomer (packed or unpacked). The reactor was filled with a NaCl 0.15N solution. HCl 1N aliquot (1.0 mL) was injected in the downcomer's middle zone (in the opposite side of the pH sensor location), and the pH changes in the riser and downcomer were followed by recording with a digital video camera (Panasonic 3CCD, 3.0 Mega Pixel, Japan) the values displayed on each potentiometer digital screen. After each experiment, the liquid in ALR was drained; and after rinsing, the reactor was filled to a predetermined liquid volume V_L. When the reactor was operated as PB-ALR, the acid retained by support material was eliminated by draining and rinsing the bed support three times; then, the reactor was filled again with NaCl 0.15 N.

The transitory changes in the relative values of pH (ΔpH[t]) in the riser, and in the packed or unpacked downcomer, were estimated with the following relation:

$$\Delta\text{pH}[t] = \frac{\text{pH}[t] - \text{pH}_0}{\text{pH}_0 - \text{pH}_\infty}$$

Those values were used to compare the dynamic tracer response profiles in both reactor configurations (ALR and PB-ALR). By plotting downcomer's $\Delta\text{pH}_D[t]$ data, the t_{m95} (95% of the change in ΔpH_D interpolated in the experimental curve) was estimated for each value of U_{GR} used.

2.6.2. Gas holdup determination in ALR and PB-ALR

The overall gas holdup was measured in the unpacked and in the packed-bed reactor using the volume expansion method [32], and calculated by:

$$\varepsilon_G = \frac{\Delta V}{\Delta V + V_{LS}} \quad (6)$$

where V_{LS} represents either the liquid-solid volume in the packed-bed system (PB-ALR) or the liquid volume in the unpacked system (ALR). ΔV is the volume expansion after gas dispersion, calculated from the average liquid level change and the cross-section area of the reactor. In order to calculate ΔV, a millimetric scale was fixed to the external glass column. Using a digital video camera (Panasonic 3CCD, 3.0 Mega Pixel, Japan), the liquid level at each gas flow rate was recorded. The registered height values from 50 frames were used to estimate the average liquid height at each gas flow rate.

2.7. Bioreactor oxygen mass transfer coefficients determination in ALR and PB-ALR

The oxygen mass transfer coefficients in riser and downcomer (unpacked or packed with the porous support) were determined in absence of bioreaction (abiotic system) using the classical dynamic gassing-in method [33]. The oxygen absorption rate in the liquid phase (NaCl 0.15N) was measured by using a calibrated DO system (YSI Inc., USA), provided with a high sensitivity membrane (YSI Model 5766) for the oxygen electrode. For k_La measurements, the oxygen electrode was located at two heights of the packed or unpacked downcomer (k_La_D) and in the net tube riser (k_La_R).

At the beginning of each experiment, nitrogen gas was bubbled to strip the dissolved oxygen from the liquid phase; then, a preadjusted airflow was fed into the riser. The change in dissolved oxygen concentration in the liquid phase C_L was followed by recording the electrode response displayed on the DO-meter's digital screen with a digital video camera (Panasonic 3CCD, 3.0 Mega Pixel, Japan). Assuming that membrane resistance of the DO sensor is negligible, the oxygen balance in the reactor was expressed in its integrated form as:

$$\mathrm{Ln}(C_S - C_L) = -k_La t + \ln(C_S - C_{L0}) \quad (7)$$

where C_S is the saturated DO concentration, C_L and C_{L0} are the bulk DO concentration at time t and $t_0 = 0$, respectively. The zonal values of k_La in each experiment were obtained from the slope of the plotted data of $\ln(C_S - C_L)$ against t.

2.8. Microbial cultivation in the PB-ALR

Initially, it was conducted a 72 h batch test to evaluate the abiotic removal of phenol and 2,4,6-TCP in the packed-bed reactor. The air flow rate Q_{AIR} was maintained at 8 L min^{-1}, corresponding to a U_{GR} value of 5.61 cm s^{-1}. Once concluded the abiotic test, the PB-ALR was inoculated with a suspension of the mixed microbial community, beginning a 72 h batch biodegradation process. Then, the reactor was operated in continuous regime, using a peristaltic pump (Masterflex, Cole Parmer, USA) for fresh medium addition, varying the operative conditions and the medium composition as described in Table 2. The dry weight of porous support was 3.647 kg and the operating volume was maintained at 4.63 L.

2.9. Analytical methods

2.9.1. Chlorides

Chloride release was determined by using the method No. 8113 from Hach Co. [34].

2.9.2. Phenol and 2,4,6-trichlorophenol

Phenol and 2,4,6-TCP were determined by column liquid chromatography using a Beckman HPLC System equipped with an Alltech Econosphere C8 reverse-phase column (150 × 4.6 mm, with particle size 5 μm) and a diode-array detector (UV 280 nm). The mobile phase consisted of two solutions: (A) H_2O + 3% CH_3COOH, and (B) methanol + 3% CH_3COOH. The volumetric proportion was 50:50. The column was operated under isocratic elution at a flow rate of 1.5 mL min^{-1}. Under these operational conditions, the phenol and TCP peaks appear at 1.5, and 2.9 min, respectively.

2.9.3. Biomass immobilized in porous support

Attached viable-biomass was determined by viable cell counting (CFU [g porous dry support]$^{-1}$). Once continuous culture runs were finished; top, medium and bottom zones of the packed bed were sampled. Cells were water-extracted from volcanic stone samples with the aid of a Vortex agitator. Stone fragments were washed and rinsed until a clear extract was obtained; then, appropriated dilutions of the collected cell suspension were used for plate counting. Another aliquot was used for cell protein determination by Lowry method [35].

2.9.4. COD determination

A closed reflux method [34] was used for COD determination. The reactive kit used could determine COD levels from 3 to 150 ppm.

2.9.5. Adsorption of 2,4,6-TCP in porous support

At the end of continuous runs carried out in the PB-ALR, samples of porous support were extracted in a vortex tube shaker using methanol as extraction solvent. The extracts were analyzed by HPLC, using a standard of 2,4,6-TCP.

2.10. Microscopic methods

Fragments of volcanic stone containing the microbial biofilm were sampled at various points of the packed bed and broken

Table 2
Operative conditions of the packed-bed bioreactor containing a microbial community immobilized in porous support

Phase number	Liquid flow rate, F_L (L d^{-1})	Dilution rate, D (d^{-1})	Input concentration (mg L^{-1})			Volumetric loading rates (mg L^{-1} d^{-1})			Chloride input, Cl_{in} (mg L^{-1})
			C_{Phe}	C_{TCP}	C_{COD}	$B_{V,Phe}$	$B_{V,TCP}$	$B_{V,COD}$	
1 (144 h)	2.59	0.56	91.70	25.10	251.40	51.25	14.03	140.50	13.53
2 (120 h)	1.10	0.24	91.70	25.10	251.40	21.73	5.95	59.57	13.53
3 (144 h)	1.10	0.24	–	25.08	22.90	–	5.94	5.43	13.53
4 (120 h)	1.18	0.25	–	68.50	66.20	–	17.36	16.78	36.91
5 (144 h)	1.56	0.34	–	139.20	125.50	–	46.88	42.27	75.01

The liquid volume V_L contained in the PB-ALR was 4.64 L; the porous support mass M_{PB} was 3.647 kg; airflow rate Q_{AIR} was 8 L min^{-1}; corresponding to a U_{GR} of 5.61 cm s^{-1}; pH of entering medium was 6.5. Chloride input Cl_{in} corresponds to the input concentration of 2,4,6-TCP. Numbers in parenthesis represent the duration of each phase, in hours.

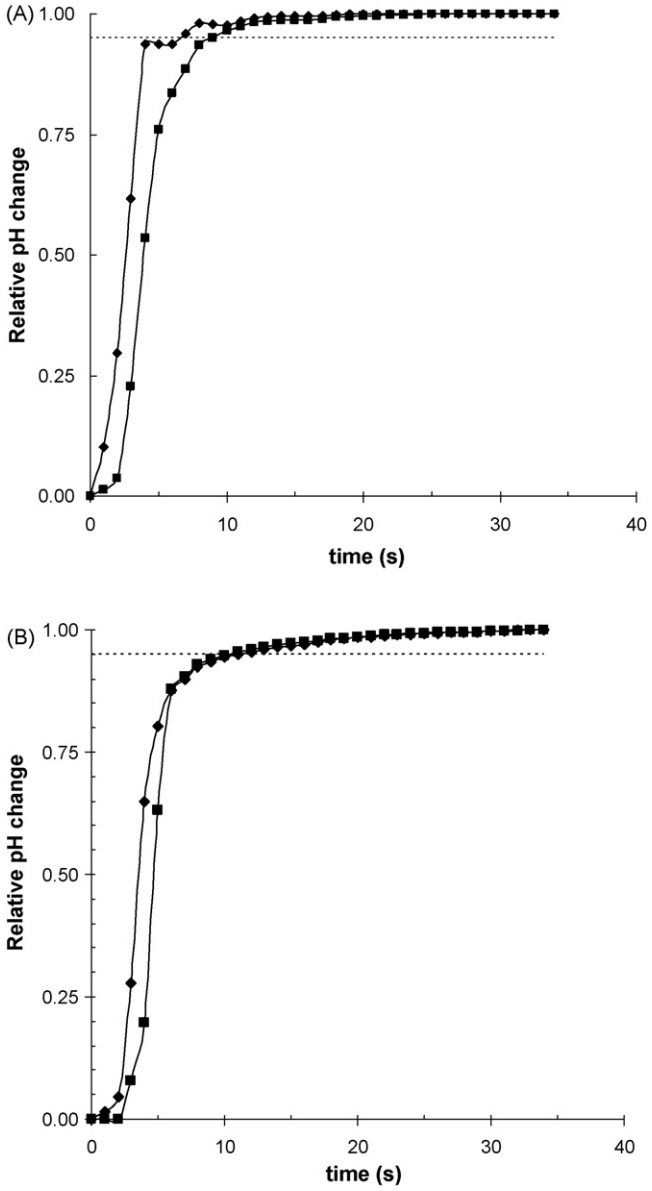

Fig. 3. Relative pH changes observed at riser (♦) and downcomer (■) in unpacked (A) or in packed-bed reactor (B). U_{GR} = 9.82 cm s^{-1}. Dotted lines show a 95% relative pH change.

into small pieces. After fixing with 2% glutaraldehide, washing twice with phosphate buffer at pH 7, post-fixing with 1% osmium, dehydrating with ethanol, drying, and finally covering with gold. Micrographs of samples were obtained in an electronic scanning microscope JEOL, JSM-5800 LV (Japan). Fig. 9 shows the vesicular structure of the porous stone and details of the attached biomass.

3. Results

3.1. Performance of the packed-bed biofilm reactor equipped with an airlift system for liquid circulation and oxygenation

3.1.1. Mixing time in ALR and PB-ALR

When using a wire-mesh tube riser, dynamic tracer response profiles distinctive from the characteristic sinusoidal profiles observed in conventional airlift reactors [36] were obtained. The profiles observed in Fig. 3A for the unpacked reactor could be explained by the hydraulic permeability of the wire-mesh riser allowing the free fluid circulation (axial and radial flow). In addition, when the downcomer was packed with irregular stone fragments acting as static mixers (Fig. 3B), only a slight delay in tracer response was observed. This delay could be explained by a diminution in liquid circulation rate and because an enhanced dispersion, originated by frictional resistance and bed tortuosity, could take place [37]. When PB-ALR's mixing time values obtained at several values of U_{GR} were compared to those obtained with the unpacked reactor (operating as an internal airlift reactor), an increase in t_{m95} at U_{GR} values higher than 3.5 cm s^{-1} (Fig. 4) was observed, inferring a diminution in liquid circulation rates caused by the interference of the porous support material.

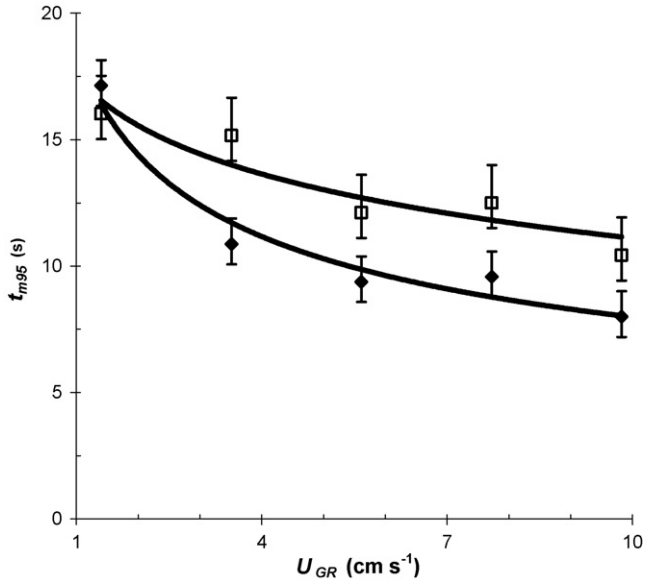

Fig. 4. Mixing time behavior in packed (□) or unpacked (♦) bed reactor.

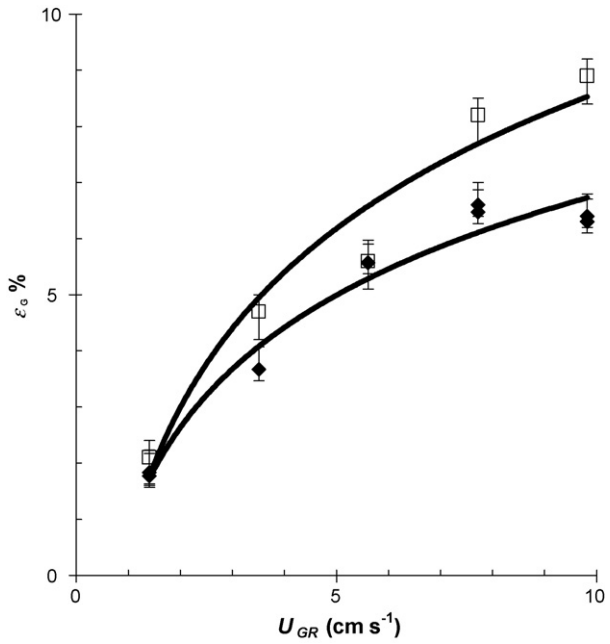

Fig. 5. Overall gas hold-up in packed (□) or unpacked (♦) bed reactor.

3.1.2. Gas holdup

A slight effect of porous packed bed on overall gas hold up profiles in PB-ALR was observed (Fig. 5). The increase in ε_G values was more noticeable at U_{GR} values higher than 7.72 cm s^{-1}. The higher retention time of gas bubbles could be originated by the diminution in liquid circulation rate, which reduces the ascending velocity of gas bubbles in the riser. An increase in overall gas holdup could also affect the gas–liquid interfacial area and thus the oxygen mass transfer coefficients.

3.1.3. Oxygen mass transfer coefficients in ALR and PB-ALR configurations

A noteworthy increase in k_La values was evidenced when reactor's downcomer was packed with porous support material. Fig. 6 shows reactor's zonal differences in oxygen transfer coefficient values when downcomer was packed with volcanic stone. The observed increase in k_La_R and k_La_D values could be caused by the reduction of downcomer's hydraulic cross-sectional area, or simply because downcomer contains less liquid volume when packed. Although there were zonal differences in the packed bed, the lowest k_La_D values obtained (higher than 40 h^{-1}) were enough to maintain an oxygen transfer rate of about 0.24 kg O_2 m^{-3} h^{-1}, adequate to oxygenate the biofilm attached to the solid fragments located at the deeper zone of the packed bed.

3.2. Phenol and 2,4,6-TCP removal in the PB-ALR

In the batch test conducted to evaluate the abiotic removal of phenol and 2,4,6-TCP, after 48 h, it was observed a plateau of about 15% in their removal efficiency (Fig. 7). Once this test was concluded, the reactor was inoculated with the mixed microbial culture, beginning a batch biodegradation process which allowed the bacterial colonization of the porous support.

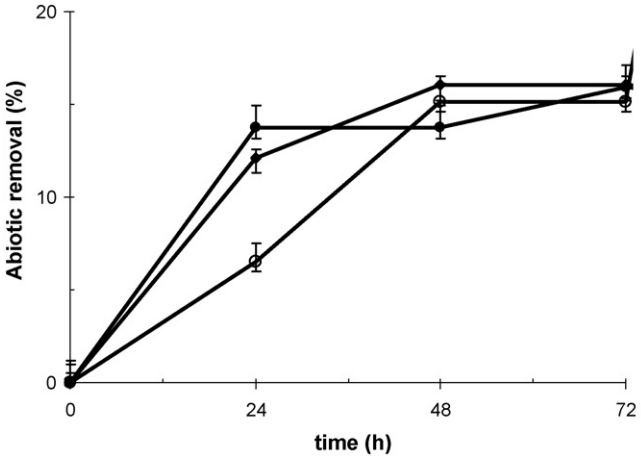

Fig. 7. Abiotic batch removal of COD (♦), phenol (●) and 2,4,6-TCP (O) in PB-ALR.

Table 3 summarizes steady-state results obtained from continuous operation of the PB-ALR corresponding to the operative conditions shown in Table 2 for five continuous runs. Initially, phenol was fed to the reactor as the primary substrate (runs 1–2). In both runs, removal efficiencies of 100% for phenol η_{Phe}, and about 98% for 2,4,6-TCP η_{TCP} were observed. The dechlorination efficiency η_{Cl} was around 80% and COD removal values η_{COD} were higher than 93%. In the third run, when 2,4,6-TCP was fed as the sole carbon and energy source, the value of η_{Cl} remained without change, and the trichlorophenol removal efficiency was higher than 99%. However, an evident decay in η_{COD} was observed (≈60%). Among all experiments carried out, this particular run had the lowest volumetric 2,4,6-TCP ($B_{V,TCP}$ = 5.94 mg L^{-1} d^{-1}) and

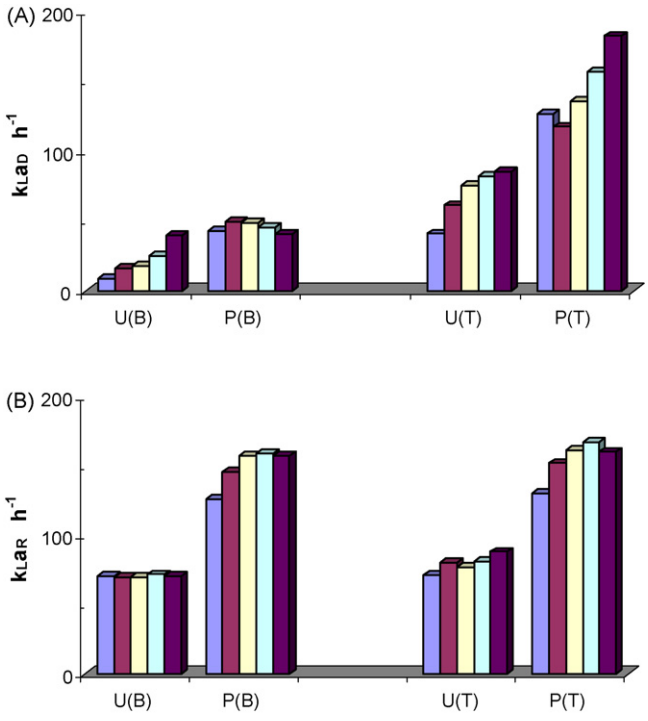

Fig. 6. Oxygen mass transfer coefficients in packed (P) or unpacked (U) reactor operating at U_{GR} values ranging from 1.4 to 9.82 cm s^{-1}. (A) k_La_D at bottom (B) and top (T) of downcomer; (B) k_La_R at bottom (B) and top (T) of riser. Color bars represent k_La values obtained at superficial air rates U_{GR} ranging from 1.4 to 9.82 cm s^{-1}. Standard deviation for k_La determinations ranged from 2.3 to 14.8%.

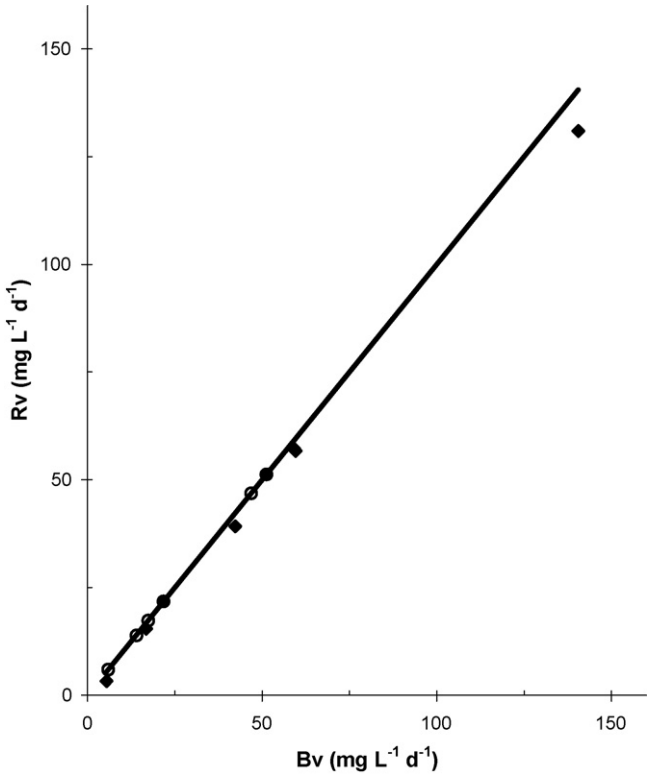

Fig. 8. Volumetric removal rates of COD (♦), phenol (●) and 2,4,6-TCP (O) in PB-ALR.

Table 3
Steady state results obtained with the PB-ALR, by using the operative conditions shown in Table 2

Phase number	Phenol, 2,4,6-TCP, COD and chloride concentrations at steady state (mg L^{-1})				Volumetric removal rates (mg L^{-1} d^{-1})			Phenol, 2,4,6-TCP, COD removal efficiencies and dechlorination efficiency (%)			
	$\tilde{c}_{Phe}$	$\tilde{c}_{TCP}$	$\tilde{c}_{COD}$	$\tilde{c}_{Cl}$	$R_{V,Phe}$	$R_{V,TCP}$	$R_{V,COD}$	η_{Phe}	η_{TCP}	η_{COD}	η_{Cl}
1 (144 h)	n.d.	0.32	17.10	10.80	51.25	13.85	130.94	100.00	98.73	93.20	79.84
2 (120 h)	n.d.	0.32	12.20	10.80	21.73	5.87	56.68	100.00	98.73	95.15	79.84
3 (144 h)		0.10	9.15	10.80	–	5.92	3.78	–	99.60	60.04	79.84
4 (120 h)		0.15	5.40	36.60	–	17.33	15.41	–	99.78	91.84	99.15
5 (144 h)		0.14	9.14	66.70	–	46.83	39.19	–	99.90	92.72	88.92

n.d.: not detectable.

COD ($B_{V,COD}$ = 5.43 mg L^{-1} d^{-1}) loading rates. Although an attached biofilm could resist oligotrophic conditions [1], the starved biomass deprived from their primary substrate (phenol) could have presented a combination of cell lysis and extracellular matrix degradation [38]. Thus, the assumed released compounds could have interfered in the COD determination.

In the fourth run, the volumetric loading rate of 2,4,6-TCP (expressed as $B_{V,TCP}$ or as $B_{V,COD}$) was almost triplicated without diminution in η_{TCP}. The η_{COD} values reached values near to 92%, and dechlorination efficiency was increased to about 99%. In the last run (5); the 2,4,6-TCP volumetric loading rate was once more increased. Again, it was not observed any diminution in η_{TCP}. The η_{COD} values remained nearly unchanged (92.72%); but, dechlorination efficiency decayed to about 89%, possibly revealing a microbial-biofilm's reduced ability to completely degrade some chlorinated byproducts not detected by HPLC.

Fig. 8 shows the removal rates $R_{V,Phe}$, $R_{V,TCP}$, and $R_{V,COD}$, obtained at various loading rates. It could be observed that under these parameters, the PB-ALR had an adequate performance; however, the diminution in dechlorination efficiency obtained at the highest loading rate probed ($B_{V,TCP}$ = 46.88 mg L^{-1} d^{-1}), possibly reveals the real 2,4,6-TCP biodegradation limit of the bacterial biofilm composed by *Stenotrophomonas* sp., *B. kururiensis*, and *Burkholderia* sp. in our bioreactor.

In the last run, once that cell plate counting and cell protein of attached biomass to porous support were determined, an overall value for the specific TCP removal rate $R_{X,TCP}$ was estimated. This term can be expressed on CFU or protein basis. The maximum estimated values were 1.807 [mg TCP (10^9 CFU)$^{-1}$ d^{-1}] or 0.831 [mg TCP (mg cell protein)$^{-1}$ d^{-1}].

3.3. Biomass distribution in the packed-bed reactor

Table 4 summarizes reactor's zonal differences in cell protein content and culturable cell plate counting from biofilm attached to porous volcanic fragments located at three packed-bed levels. In both terms a relative homogeneity along the packed bed could be appreciated. This behavior is in correspondence with the absence of anoxic or starved zones in PB-ALR, corroborated by the oxygen mass transfer rates supporting an adequate oxygenation of the attached biofilm located at the sampled zones of the downcomer, and by the dynamic tracer response profiles obtained in the packed-bed reactor. In Fig. 9A the porous structure of tezontle fragments could be observed, and the biofilm formed in a vesicular cavity could be appreciated in Fig. 9B–C.

Table 4
Culturable cell plate counting and cell protein distribution in packed-bed porous support

Sampled zone of packed bed	Culturable cell plate counting CFU (g support)$^{-1}$	Cell protein content mg (g support)$^{-1}$
Top	$1.47 \times 10^7 \pm 34.08\%$	$0.0356 \pm 35.48\%$
Medium	$2.38 \times 10^7 \pm 31.01\%$	$0.0559 \pm 36.97\%$
Bottom	$2.14 \times 10^7 \pm 24.30\%$	$0.0385 \pm 21.30\%$

3.4. Adsorption of 2,4,6-TCP in porous support

2,4,6-TCP was not detected by HPLC in methanol-extracts of porous support samples obtained from three levels of the packed bed. Hence, it was corroborated that biodegradation was the main mechanism for 2,4,6-removal in PB-ALR.

4. Discussion

It has been reported that a cross flow design reduces pressure drop enabling the use of practical flow rates and even distribution of flow across the wide packed bed [8]. The cross flow (radial flow) diminishes the substrate solution linear velocity through the packed bed with the consequent increase in hydraulic retention time. In addition, it reduces gradient concentration formation and pressure drop, particularly with low height packed beds. The net draft tube riser produces a liquid circulation pattern distinct to that observed in conventional airlift reactors (upward-flow and downward-flow zones). When net or perforated draft tube risers are used in non-conventional airlift reactors, additionally to axial flow, radial flow is produced [39,40]. This circulation pattern influences the oxygen mass transfer coefficient (Fig. 6A) and the mixing performance in the packed bed, revealed by the dynamic tracer response profiles (Fig. 3). In addition, due to the separation of the aeration zone (net draft tube) from the packed bed, the hybrid PB-ALR bioreactor should present low shear stress [41].

Considering the oxygen transfer rate as a useful indicator of chemical substances distribution into the packed bed, the t_{m95} values obtained with the PB-ALR configuration, the 2,4,6-TCP biodegradation rates at the volumetric loading rates probed, and the zonal values of biomass attached to porous volcanic fragments, it can be assumed that the biofilm growth was not limited by oxygen in the packed-bed sampled zones.

Although the amount of attached biomass determined by viable cell plate counting and cell-protein content was relatively low, the elevated 2,4,6-TCP dechlorination and COD removal efficiencies, joined to the null detection of trichlorophenol adsorbed to the porous support, showed that biodegradation was the main mechanism for 2,4,6-TCP removal in the PB-ALR.

Microbial degradation of a highly halogenated phenol requires enough energy to carry out its dehalogenation, particularly when chlorine is the substituent, due to the high bond energy of the carbon–chlorine linkage [42]. In addition, as chlorophenols are potent uncouplers of oxidative phosphorylation, collapsing cell's proton motive force; still more energy is needed to carry out their biodegradation [43].

In this work, phenol was initially used as primary energy source to co-metabolically degrade 2,4,6-TCP. However, the ability of the mixed bacterial culture to metabolize 2,4,6-TCP in absence of phenol was also observed in the biofilm reactor.

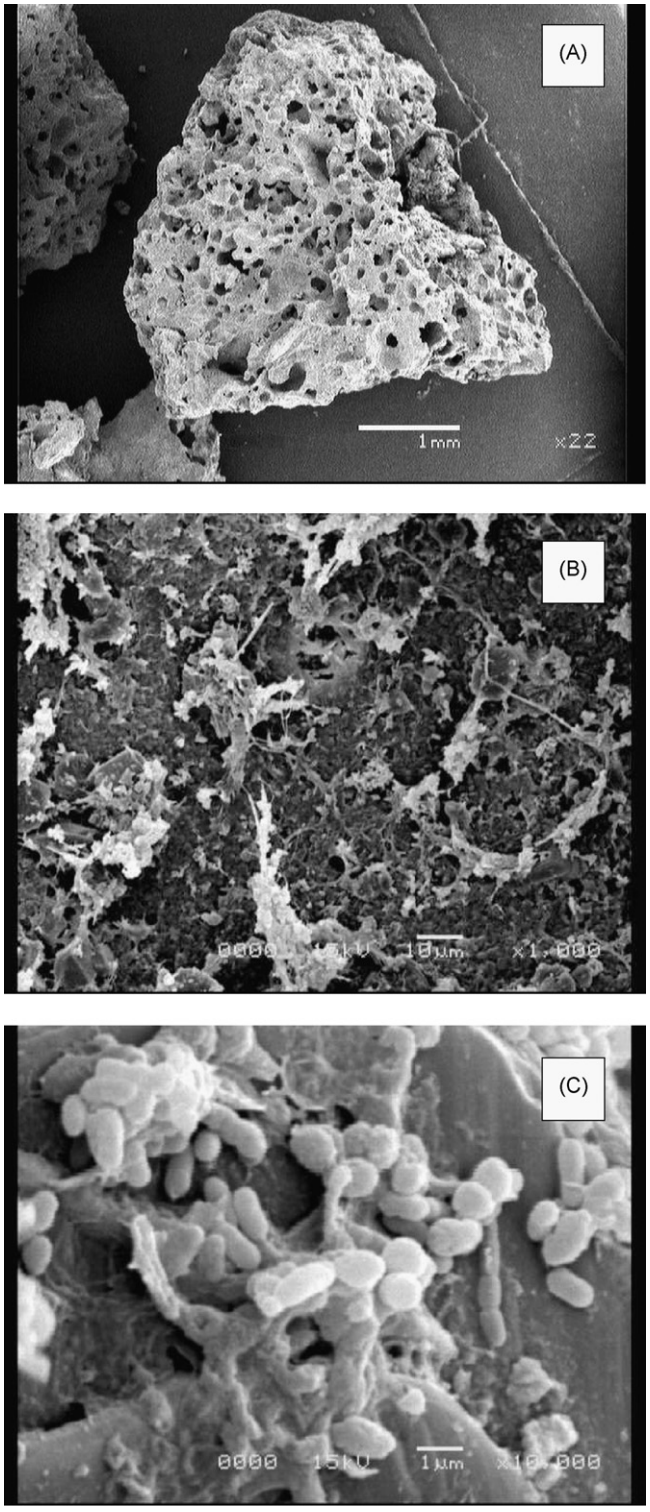

Fig. 9. Fragment of tezontle: (A) vesicular structure; (B) bacterial biofilm in a vesicular cavity; (C) detail of bacteria in biofilm.

The ability of a microbial consortium to degrade a recalcitrant compound without supplying an external primary substrate could have several explanations, all of them sustained in a possible change of the primary energy source used by microbial cells.

(i) Although an attached biofilm could resist oligotrophic conditions in absence of a primary energy source [1], the starved biofilm deprived from their primary substrate could release materials by cell lysis [38], providing primary substrates for TCP cometabolism. (ii) Because mature microbial biofilms contain external polymeric substances (EPS) [44], synthesized when an excess of the primary carbon source was available, EPS could also provide an external energy source for the co-metabolic biodegradation of TCP [45]. (iii) It has been reported that co-metabolic biodegradation of halophenols take place only when the microorganism has enough energy reserves [42], and that consumption of cell's reserve materials occurs during 2,4,6-TCP degradation [46], thus, reserve material could also be used as primary substrates to carry out co-metabolic processes.

On the other hand 2,4,6-TCP biodegradation by pure or mixed cultures in absence of external energy sources has been reported. By the white rot fungi *Phanerochaete chrysosporium* [47], by indigenous microbial biomass grown in sand-bed columns [50], and by the genera *Alcaligenes* [48], *Sphingomonas*, *Pseudomonas*, *Azotobacter*, *Novosphingobium* and *Arthrobacter* [49]

5. Conclusions

The characteristics of this support material; size, irregular shape, and porosity, joined to its mechanical resistance, allowed an internal radial flow driven by the difference in hydrostatic pressure between the net tube riser and the packed downcomer. In addition, the PB-ALR configuration (low H_{PB}/D_C and high A_D/A_R ratios) and the use of a net draft tube for liquid oxygenation and circulation supports higher oxygen mass transfer rates and comparable system's mixing-time than that obtained with the unpacked reactor. The liquid velocities pattern created by radial flow through the porous support could reduce the biofilm erosion since the higher shear stress occurs into the riser.

The attached bacterial consortium removed 100% of phenol and near 99% of 2,4,6-TCP when phenol was used as primary substrate. Mineralization and dehalogenation of 2,4,6-TCP was evidenced by high COD removal efficiencies (≈95%), and by the stoichiometric release of chloride ions from the halogenated compound (≈80%). Finally, it was observed that the microbial consortium was also capable to metabolize 2,4,6-TCP without phenol as primary substrate, with high removal efficiencies (near 100% for 2,4,6-TCP, 92% for COD and 88% for chloride ions)

References

[1] S.H. Israni, S.S. Koli, A.W. Patwardhan, J.S. Melo, S.F. D'souza, Phenol degradation in rotating biological contactors, J. Chem. Technol. Biotechnol. 77 (2002) 1050–1057.
[2] G. Tziotzios, M. Teliou, V. Kaltsouni, G. Lyberatos, D.V. Vayenas, Biological phenol removal using suspended growth and packed bed reactors, Biochem. Eng. J. 26 (2005) 65–71.
[3] S.-Y. Lee, Y. Pang-Tsui, Succeed at gas/liquid contacting, Chem. Eng. Prog. 95 (1999) 23–49.
[4] J. Pérez, J.L. Montesinos, F. Gòdia, Gas-liquid mass transfer in an up-flow cocurrent packed-bed biofilm reactor, Biochem. Eng. J. 31 (2006) 188–196.
[5] G. Radilla, M. Fourar, F. Larachi, Correlating gas-liquid co-current flow hydrodynamics in packed beds using the F-function concept, J. Chem. Technol. Biotechnol. 80 (2005) 107–112.
[6] B.A. Meyer, D.W. Smith, Flow through porous media: comparison of consolidated and unconsolidated materials, Ind. Eng. Chem. Fundam. 24 (1985) 360–368.
[7] H.-J. Jördening, K. Buchholz, Fixed film stationary bed and fluidized bed reactors, in: I.J. Winter (Ed.), Biotechnology, vol. 11a: Environmental Processes, Wiley-VCH Weinheim, Germany, 1999.
[8] S.K. Ajmera, C. Delattre, M.A. Schmidt, K.F. Jensen, Microfabricated cross-flow chemical reactor for catalyst testing, Sens. Actuators, B: Chem. 82 (2002) 297–306.
[9] C.-C. Fu, W.-T. Wu, S.-Y. Lu, Performance of airlift reactors with net draft tube, Enzyme Microbial. Technol. 33 (2003) 332–342.
[10] J.A. Rintala, J.A. Puhakka, Anaerobic treatment in pulp and paper-mill waste management: a review, Bioresource Technol. 47 (1994) 1–18.

[11] G.W. Holcombe, G.L. Phipps, A.H. Sulaiman, A.D. Hoffman, Simultaneous multiple species testing: acute toxicity of 13 chemicals to 12 diverse freshwater amphibian, Fish, and invertebrate families, Arch. Environ. Contam. Toxicol. 16 (1987) 697–710.
[12] O. Maltseva, P. Oriel, Monitoring of an alkaline 2,4,6-trichlorophenol-degrading enrichment culture by DNA fingerprinting methods and isolation of the responsible organism, *Haloalkaliphilic nocardioides* sp. strain M6, Appl. Environ. Microbiol. 63 (1997) 4145–4149.
[13] M. Sittig, Handbook of Toxic and Hazardous Chemicals, Noyes Publications, Park Ridge, NJ, 1981.
[14] L. Kharoune, M. Kharoune, J.M. Lebeault, Aerobic degradation of 2,4,6-trichlorophenol by a microbial consortium—selection and characterization of microbial consortium, Appl. Microbiol. Biotechnol. 59 (2002) 112–117.
[15] National Programme for the Reduction of Pollution by 2,4,6-Trichlorophenol under article 7 of directive 76/464/EEC, Edited by Environmental Resources Management, Eaton House, Wallbrook Court, North Hinksey Lane, Oxford, UK, 2002.
[16] V. Matus, M.A. Sánchez, M. Martínez, B. González, Efficient degradation of 2,4,6-trichlorophenol requires a set of catabolic genes related to tcp genes from *Ralstonia eutropha* JMP134(pJP4), Appl. Environ. Microbiol. 69 (2003) 7108–7115.
[17] I.J. Ochuma, R.P. Fishwick, J. Wood, J.M. Winterbottom, Photocatalytic oxidation of 2,4,6-trichlorophenol in water using a cocurrent downflow contactor reactor (CDCR), J. Hazard. Mater. 144 (2007) 627–633.
[18] S. Şenel, A. Kara, G. Alsancak, A. Denizli, Removal of phenol and chlorophenols from water with reusable dye-affinity hollow fibers, J. Hazard. Mater. 138 (2006) 317–324.
[19] M. Radhika, K. Palanivelu, Adsorptive removal of chlorophenols from aqueous solution by low cost adsorbent—kinetics and isotherm analysis, J. Hazard. Mater. 138 (2006) 116–124.
[20] G. Collins, C. Foy, S. McHugh, V. O'Flaherty, Anaerobic treatment of 2,4,6-trichlorophenol in an expanded granular sludge bed-anaerobic filter (EGSB-AF) bioreactor at 15 °C, FEMS Microbiol. Ecol. 53 (2005) 167–178.
[21] C. Aranda, F. Godoy, J. Becerra, R. Barra, M. Martínez, Aerobic secondary utilization of a non-growth and inhibitory substrate 2,4,6-trichlorophenol by *Sphingopyxis chilensis* S37 and *Sphingopyxis*-like strain S32, Biodegradation 14 (2003) 265–274.
[22] G.A. Ehlers, P.D. Rose, Immobilized white-rot fungal biodegradation of phenol and chlorinated phenol in trickling packed-bed reactors by employing sequencing batch operation, Bioresource Technol. 96 (2005) 1264–1275.
[23] M. Briglia, F.A. Rainey, E. Stackebrandt, G. Schraa, M.S. Salkinoja-Salonen, *Rhodococcus percolatus* sp. nov., a bacterium degrading 2,4,6-trichlorophenol, Int. J. Syst. Bacteriol. 46 (1996) 23–30.
[24] P. Clément, V. Matus, L. Cárdenas, B. González, Degradation of trichlorophenols by *Alcaligenes eutrophus* JMP134, FEMS Microbiol. Lett. 127 (1995) 51–55.
[25] D.-Y. Li, J. Eberspächer, B. Wagner, J. Kuntzer, F. Lingens, Degradation of 2,4,6-trichlorophenol by *Azotobacter* sp. strain GP1, Appl. Environ. Microbiol. 57 (1991) 1920–1928.
[26] H. Kiyohara, T. Hatta, Y. Ogawa, T. Kakuda, H. Yokohama, N. Takizawa, Isolation of *Pseudomonas pickettii* strains that degrade 2,4,6-trichlorophenol and their dechlorination of chlorophenols, Appl. Environ. Microbiol. 58 (1992) 1276–1283.
[27] S. Eker, F. Kargi, 2,4,6-Trichlorophenol containing wastewater treatment using a hybrid-loop bioreactor system, J. Environ. Eng. 133 (2007) 340–345.
[28] J.-H. Kim, K.-K. Oh, S.-T. Lee, S.-W. Kim, S.-I. Hong, Biodegradation of phenol and chlorophenols with defined mixed culture in shake-flasks and a packed bed reactor, Process Biochem. 37 (2002) 1367–1373.
[29] F.J. Romano-Baez, Desarrollo de un bioproceso para la degradación cometabólica de 2,4,6-triclorofenol, M.Sc. Thesis, Escuela Nacional de Ciencias Biológicas, Instituto Politécnico Nacional, México, 2007.
[30] D.S. Hodge, J.S. Devinny, Modeling removal of air contaminants by biofiltration, J. Environ. Eng. 121 (1995) 21–32.
[31] R.A. Bello, C.W. Robinson, M. Moo-Young, Gas holdup and overall volumetric oxygen transfer coefficient in airlift contactors, Biotechnol. Bioeng. 27 (1985) 369–381.
[32] J.M.T. Vasconcelos, J.M.L. Rodrigues, S.C.P. Orvalho, S.S. Alves, R.L. Mendes, A. Reis, Effect of contaminants on mass transfer coefficients in bubble column and airlift contactors, Chem. Eng. Sci. 58 (2003) 1431–1440.
[33] H. Taguchi, A.E. Humphrey, Dynamic measurement of the volumetric oxygen transfer coefficients in fermentation systems, J. Ferment. Technol. 44 (1966) 881–889.
[34] Hach Company, Hach Water Analysis Handbook, Colorado, USA. 1997.
[35] O.H. Lowry, N.J. Rosebrough, A.L. Farr, R.J. Randall, Protein measurement with the folin-phenol reagents, J. Biol. Chem. 193 (1951) 265–275.
[36] M.Y. Chisti, Airlift Bioreactors. Essex (GB)., Elsevier Science Publishers Ltd., 1989.
[37] A.X. Meng, G.A. Hill, A.K. Dalai, Hydrodynamic characteristics in an external loop airlift bioreactor containing a spinning sparger and a packed bed, Ind. Eng. Chem. Res. 41 (2002) 2124–2128.
[38] S.M. Hunt, E.M. Werner, B. Huang, M.A. Hamilton, P.S. Stewart, Hypothesis for the role of nutrient starvation in biofilm detachment, Appl. Environ. Microbiol. 70 (2004) 7418–7425.
[39] C.-C. Fu, S.-Y. Lu, Y.-J. Hsu, G.-C. Chen, Y.-R. Lin, W.-T. Wu, Superior mixing performance for airlift reactor with a net draft tube, Chem. Eng. Sci. 59 (2004) 3021–3028.
[40] M.Y. Chisti, Mass transfer, in: Kirk-Othmer Encyclopedia of Chemical Technology, vol. 15, 5th ed., Wiley, New York, 2005, pp. 1–75.
[41] D. Fassnacht, R. Pörtner, Experimental and theoretical considerations on oxygen supply for animal cell growth in fixed-bed reactors, J. Biotechnol. 72 (1999) 169–184.
[42] A. Papazi, K. Kotzabasis, Bioenergetic strategy for the biodegradation of phenolic compounds—exogenously supplied energy and carbon sources adjust the level of biodegradation, J. Biotechnol. 129 (2007) 706–716.
[43] A. Salmerón-Alcocer, N. Ruiz-Ordaz, C. Juárez-Ramírez, J. Galíndez-Mayer, Continuous biodegradation of single and mixed chlorophenols by a mixed microbial culture constituted by *Burkholderia* sp., *Microbacterium phyllosphaerae*, and *Candida tropicalis*, Biochem. Eng. J. 37 (2007) 201–211.
[44] J.W. Costerton, Overview of microbial biofilms, J. Ind. Microbiol. 15 (1995) 137–140;
P.L. Bishop, T.C. Zhang, Y.-C. Fu, Effects of biofilm structure, microbial distributions and mass transport on biodegradation processes, Water Sci. Technol. 31 (1995) 143–152.
[45] J.-U. Kreft, J.W.T. Wimpenny, Effect of EPS on biofilm structure and function as revealed by an individual-based model of biofilm growth, Water Sci. Technol. 43 (2001) 135–141;
V.Z. Lazarova, J. Manem, Biofilm characterization and activity analysis in water and wastewater treatment, Water Res. 29 (1995) 2227–2245.
[46] F.A. Godoy, M. Bunster, V. Matus, C. Aranda, B. González, M.A. Martínez, Poly-β-hydroxyalcanoates consumption during degradation of 2,4,6-trichlorophenol by *Sphingopyxis chilensis* S37, Lett. Appl. Microbiol. 36 (2003) 315–320.
[47] P.M. Armenante, N. Pal, G. Lewandowski, Role of mycelium and extracellular protein in the biodegradation of 2,4,6-trichlorophenol by phanerochaete chrysosporium, Appl. Environ. Microbiol. 60 (1994) 1711–2171.
[48] V. Andreoni, G. Baggi, M. Colombo, L. Cavalca, M. Zangrossi, S. Bernasconi, Degradation of 2,4,6-trichlorophenol by a specialized organism and by indigenous soil microflora: bioaugmentation and self-remediability for soil restoration, Lett. Appl. Microbiol. 27 (1998) 86–92.
[49] C. Fang, C.-M. Lee, C.-C. Wang, Degradation of chlorophenols using pentachlorophenol-degrading bacteria *Sphingomonas chlorophenolica* in a batch reactor, Curr. Microbiol. 51 (2005) 156–160.
[50] B. AntizarLadislao, N.I. Galil, Biodegradation of 2,4,6-trichlorophenol and associated hydraulic conductivity reduction in sand-bed columns, Chemosphere 64 (2006) 339–349.